Contents **Pages**

1. General methods

All starting materials were purchased from Acros Organics, Alfa Aesar, Sigma Aldrich, or TCI America and used without further purification. **NMR spectra** (^{1}H, ^{13}C, HSQC, HMBC) were collected on a 700 MHz AdvanceIII Bruker instrument at 25 °C and processed using TopSpin 3.5pl7. Chemical shifts are reported as parts per million (ppm). **Mass spectrometry:** low-resolution electrospray ionization (ESI) mass spectrometry and high-resolution (ESI) mass spectrometry was carried out at the Stony Brook University Institute for Chemical Biology and Drug Discovery (ICB&DD) Mass Spectrometry Facility with an Agilent LC/MSD and Agilent LC-UV-TOF spectrometers respectively. **UV-VIS** spectra were collected with the NanoDrop ^{1}C instrument (AZY1706045). Spectra were recorded from 200 to 900 nm in a quartz cuvette with 1 cm path length. **HPLC:** Preparative HPLC was carried out using a Shimadzu HPLC-20AR equipped with a Binary Gradient, pump, UV-Vis detector, manual injector on a Phenomenex Luna C18 column (250 mm×21.2 mm, 100 Å, AXIA packed). Method A (preparative purification method): A = 0.1% TFA in water, B = 0.1% TFA in MeCN. Gradient: 0-5 min: 95% A. 5-24 min: 5−95% B gradient. Method B (preparative purification method): A = 10^{-2} M ammonium formate in water, B = 10% 10 mM ammonium formate in water, 90% MeCN. Gradient: 0-5 min: 95% A. 5-24 min: 5−95% B gradient. RadioHPLC analysis was carried out using a Shimadzu HPLC-20AR equipped with a binary gradient, pump, UV-Vis detector, autoinjector and Laura radiodetector on a Gemini-NX C18 column (100 mm×3 mm, 110 Å, AXIA packed). Method C (analysis of L2, $[Tb(L2)]^{-}$ and $[Tb(L2)^{89}Zr]$): A = 0.1% TFA in water, B = 0.1% TFA in MeCN with a flow rate of 0.8 mL/min, UV detection at 260 and 280 nm. Gradient: 0-5 min: 95% A. 5-24 min: 5−95% B gradient. **Luminescence measurements** were carried out on a Hitachi F-7100 FL spectrophotometer. Wavelength scans were collected by exciting at the appropriate wavelength (282 nm for Tb(III), 275 nm for Eu(III)) for antenna-mediated excitation and minimization of scattering interference. Emission spectra were collected from 300 to 700 nm for terbium and 400 to 800 nm for europium, with 1.0 nm excitation and 5.0 nm emission slit width, 1200 s scan time, 0.05 s response time, PMT voltage = 400 V. Quantum yield measurements were carried out using $Ru(bipy)_3$ as standard (λ_{ex} = 450 nm). Lifetime measurements were executed using the following settings: Scan time 20 ms; chopping speed of 40 Hz; excitation wavelength of 255.0 nm and emission wavelength of 555.0 nm; 0-second delay; excitation and emission slit widths of 10 nm each; 0.5 second response. Complexes were dissolved in H_2O or D_2O (samples were resuspended and lyophilized in D_2O repeatedly prior to measurement). A quartz cuvette with a 1 cm pathlength was used. **ICP-OES** was carried out using an Agilent 5110 ICP-OES. A 10-point standard with respect to terbium, europium, and lanthanum was used and fits were found to be with R^2 of 0.9999. Concentrations were then back-calculated to the stock sample concentration. Concentrations of each lanthanide complex were diluted based on stock concentrations determined by ICP. 500 µL aliquots of dilutions were prepared in 1X DBPS buffer, to which 10 µL of isotope (10-30 µCi) was added to produce a final volume of 510 µL. Plasma studies were carried out by aliquoting 250 µL of Sprague Dawley Rat Plasma in sodium heparin from Innovative Research labs into 250 µL of lanthanide complex. **IVIS** Lumina Series II from Caliper LifeSciences small animal imager was used to image phantoms. All scans were collected with blocked excitation filter, open emission filter (from 515 nm to 840 nm) and collection time t = 5 minutes. Images were analyzed with Living Image software version 4.3.1. Regions of interest were determined in quintuplicate with the ROI tool for each concentration as well as a general background ROI for background correction.

2. Synthesis protocols and characterization

[Ln(DOTA)] and [Ln(L1)] complexes. The synthesis of DOTA and **L1** was carried out as described previously.[1,2] Complexation of all ligands was completed by dissolving ligand and lanthanide triflate salt in water at a 1.2:1 ratio. The pH of the mixture was adjusted to 7.2 by addition of 0.1 M NaOH. At pH 7.2, luminescence of Tb(III)- and Eu(III)- containing complexes was observed when excited with 245 nm light from a hand-held UV-lamp. The resulting suspension was centrifuged to remove any precipitating lanthanide salt. The supernatant was collected and lyophilized overnight, yielding the product as a white solid without any further purification.

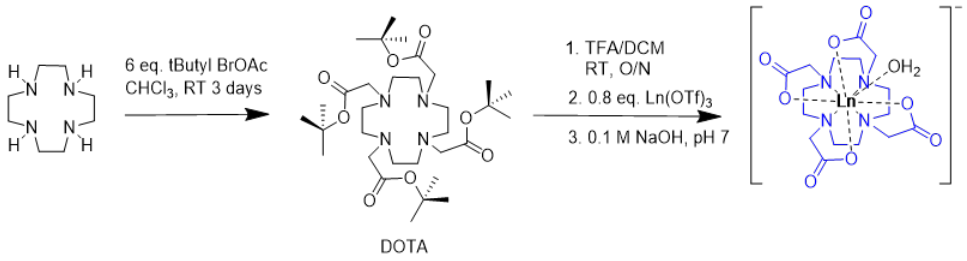

Scheme S1. Synthesis and complexation of DOTA.

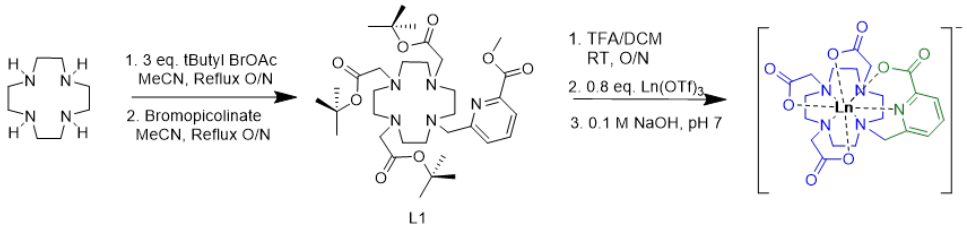

Scheme S2. Synthesis and complexation of **L1**.

2,2',2"-(10-((6-Carboxypyridin-2-yl)methyl)-1,4,7,10-tetraazacyclododecane-1,4,7-triyl)triacetic Acid, **L1:** ^{1}H NMR (D_2O, 700 MHz): 8.25 (s, 2H, py), 8.06 (s, 1H, py), 4.43-2.73 (m, 24H, CH_2). ESI-MS calcd. for $C_{21}H_{31}N_5O_8^+$: 481.22. Found: 482.4 $[M+H]^+$.

1,4,7,10-Tetraazacyclododecane-1,4,7,10-tetraacetic acid, DOTA: ^{1}H NMR (D_2O, 700 MHz, 25 °C): 4.01-3.31 (br, 8H, NCH_2COO), 3.19-2.32 (m, 16H, NCH_2CH_2N). ESI-MS calcd. for $C_{16}H_{28}N_4O_8^+$: 404.42. Found: 405.1 $[M+H]^+$.

Na[Tb(DOTA)]: Yield 124 mg (66%); ESI-MS calcd. for $C_{16}H_{24}TbN_4O_8^-$: 559.1. Found: 549.0 $[M]^-$.

Na[Eu(DOTA)]: Yield 151 mg (84%); ESI-MS calcd. for $C_{16}H_{24}EuN_4O_8^-$: 553.1. Found: 554.0 $[M]^-$.

Na[La(DOTA)]: Yield 145 mg (80%); ^{1}H NMR (D_2O, 700 MHz): 4.01-3.31 (m, 8H, NCH_2COO), 3.19-2.32 (m, 16H, NCH_2CH_2N). ESI-MS calcd. for $C_{16}H_{24}LaN_4O_8^-$: 539.1. Found: 539.0 $[M]^-$.

Na[Tb(**L1**)]: Yield 22.0 mg (54%); ESI-MS calcd. for $C_{21}H_{27}TbN_5O_8^-$: 636.1. Found: 636.0 $[M]^-$.

Na[Eu(**L1**)]: Yield 15.0 mg (37%); ESI-MS calcd. for $C_{21}H_{27}EuN_5O_8^-$: 630.1. Found: 630.0 $[M]^-$.

Na[La(**L1**)]: Yield 31.0 mg (78%); ^{1}H NMR (D_2O, 700 MHz): 8.20 (t, 1H, py), 8.07 (d, 1H, py), 7.78 (d, 1H, py), 3.99-2.91 (m, 24H, CH_2). ESI-MS calcd. for $C_{21}H_{27}LaN_5O_8^-$: 616.1. Found: 616.1 $[M]^-$.

2.B Synthesis of DFO-conjugated chelator **L2**:

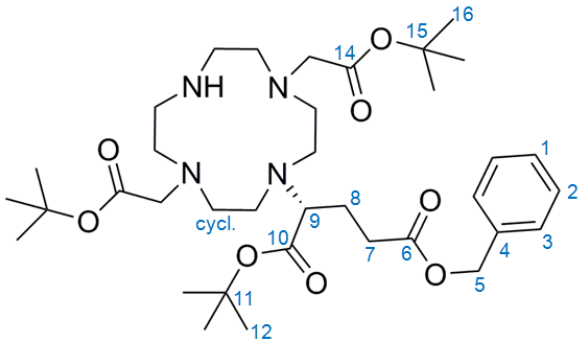

2-(R)-2-(7,10-Bistert-Butyloxycarbonylmethyl-1,4,7,10-tetraazacyclododec-1-yl)-pentanedioic Acid-1-tert-Butyl-5-benzyl Ester, 2. 5-Benzyl 1-(tert-butyl) (S)-2-((methylsulfonyl)oxy)pentadioate (300 mg, 0.80 mmol) was synthesized according to literature procedure[3], and added to a solution of 1,4,7,10-tetraazacyclododecane-1,7-diacetic acid (DO2A, 200 mg, 0.50 mmol) and K_2CO_3 (69 mg, 0.50 mmol) in acetonitrile (15 mL). The mixture was refluxed overnight. Upon completion as confirmed by LC-MS, the mixture was filtered, and the filtrate was purified using preparative HPLC (method A), with the product eluting at 17.5 minutes. The fractions containing product were pooled and the solvent was removed in vacuo to afford **2** as colorless oil (79.9 mg, 0.12 mmol, 15% yield, R_t (method C) =10.45 min). ^{1}H NMR (CD_3OD, 700 MHz): δ 7.37 (m, 5H, $H^{1,2,3}$), 5.17 (s, 2H, H^5), 4.41 (m, 1H, H^9), 3.66 (m, 8H, H^{cycl}), 3.39 (m, 4H, H^{cycl}), 3.20 (m, 4H, H^{cycl}), 2.86 (m, 2H, H^7), 2.76 (m, 4H, H^{13}), 2.36 (m, 1H, H^8), 2.16 (m, 1H, H^8), 1.58 (s, 9H, H^{12}), 1.48 (s, 18H, H^{16}); ^{13}C NMR (CD_3OD, 175 MHz): δ 174.43 (C^{14}), 172.76 (C^6), 170.64 (C^{10}), 135.92 (C^4), 128.29 (C^2), 128.12 (C^1), 128.08 (C^3), 86.12 (C^{11}), 81.87 (C^{15}), 66.42 (C^5), 61.58 (C^9), 54.82 (C^{cycl}), 54.26 (C^{cycl}), 52.14 (C^{13}), 44.96 (C^{cycl}), 42.30 (C^{cycl}), 29.99 (C^7), 27.05 (C^{12}), 26.95 (C^{16}), 19.74 (C^8). ESI-MS: calcd. for $C_{36}H_{61}N_4O_8^+$: 677.4484. Found: 677.4492 $[M+H]^+$.

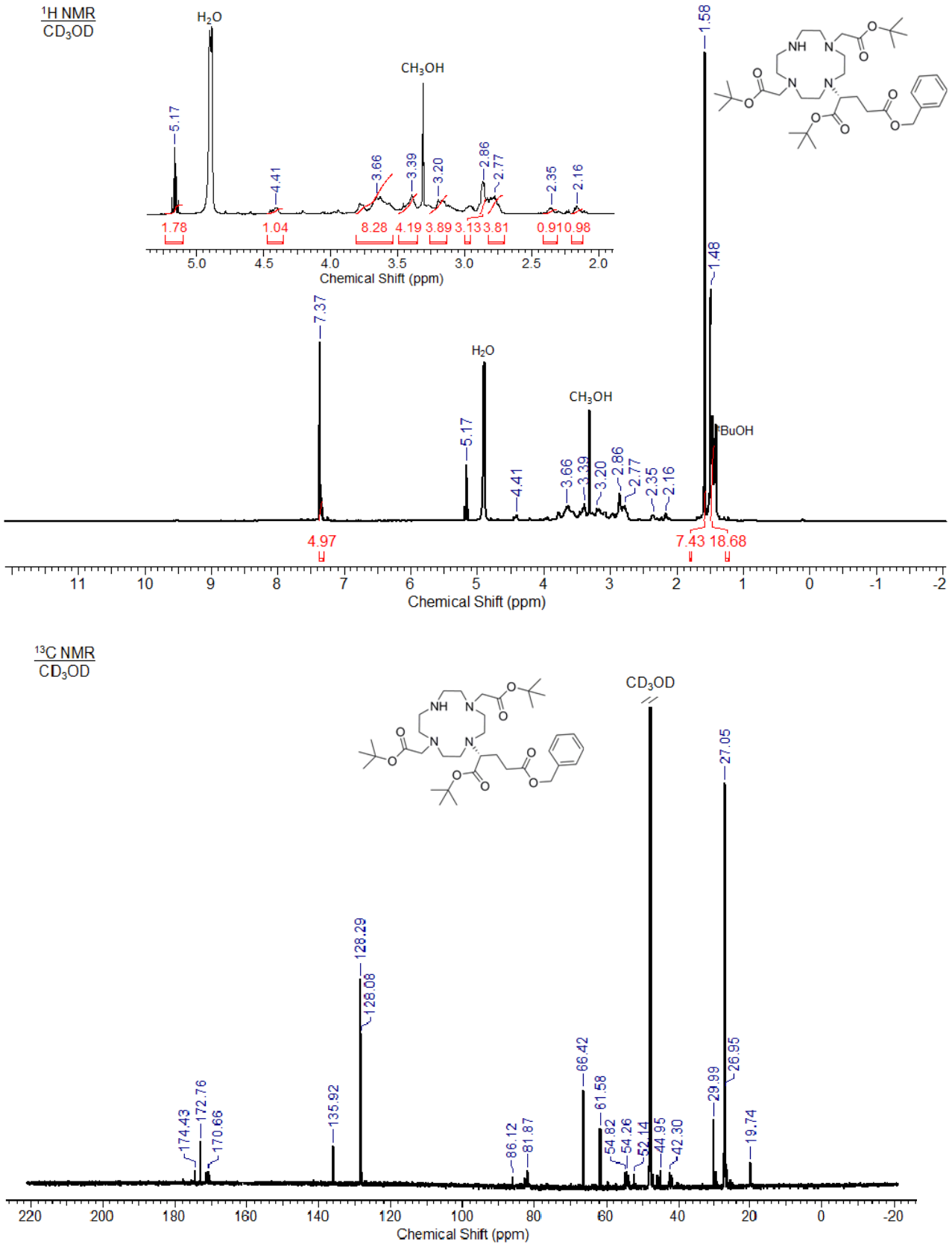

Figure S1. ^{1}H (top) and ^{13}C (bottom) NMR spectra of **2**.

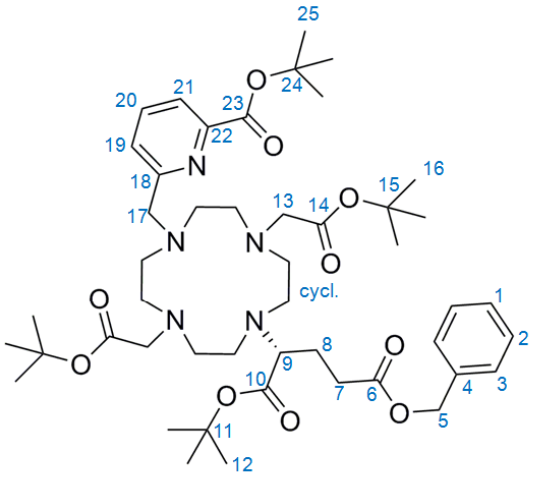

2-(R)-2-(7,10-Bistert-Butyloxycarbonylmethyl-(6-Carboxypyridin-2-yl)tert-butyl)-1,4,7,10-tetraazacyclododec-1-yl)-pentanedioic Acid-1-tert-Butyl-5-benzyl Ester, 4. To a solution of **2** (27.9 mg, 0.041 mmol) dissolved in 5 mL of acetonitrile, K_2CO_3 (5.7 mg, 0.04 mmol) and **3** (8.2 mg, 0.030 mmol) were added, and the reaction was stirred overnight at room temperature. Subsequently, the mixture was filtered and the volume of filtrate was reduced to 2 mL in vacuo. The concentrated solution was then purified using HPLC and method A, with the product eluting at 20.5 minutes. The fractions containing the desired product were pooled and the solvent was removed in vacuo to afford **4** as white powder (18.2 mg, 0.021 mmol, 69% yield, R_t (method C) = 7.42 min). Unreacted starting material was also recovered. ^{1}H NMR (CD_3OD, 700 MHz): δ 8.01 (m, 1H, H^{21}), 7.80 (m, 1H, H^{20}), 7.36 (m, 6H, H^1, H^2, H^3, H^{19}), 5.16 (s, 2H, H^5), 4.46 (m, 1H, H^9), 3.98 (s, 2H, H^{17}), 3.72 (m, 8H, H^{cycl}), 3.47 (m, 4H, H^{cycl}), 3.22 (m, 4H, H^{cycl}), 2.86 (m, 2H, H^7), 2.80 (br. s, 4H, H^{13}), 2.22 (m, 1H, H^8), 1.98 (m, 1H, H^8), 1.64 (s, 9H, H^{12}), 1.49 (s, 18H, H^{16}), 1.42 (s, 9H, H^{25}). ^{13}C NMR (CD_3OD, 175 MHz): δ 174.69 (C^{14}), 173.23 (C^6), 170.30 (C^{10}), 163.03 (C^{23}), 159.03 (C^{18}), 149.43 (C^{22}), 139.80 (C^{20}), 137.32 (C^4), 129.44 (C^2), 129.35 (C^1), 129.30 (C^3), 126.22 (C^{19}), 125.24 (C^{21}), 83.83 (C^{11}), 82.62 (C^{15}), 82.01 (C^{24}), 67.53 (C^5), 61.54 (C^9), 57.90 (C^{cycl}), 55.80 (C^{cycl}), 55.60 (C^{cycl}), 53.965 (C^{cycl}), 53.05 (C^{13}), 50.19 (C^{17}), 28.57 (C^{25}), 28.46 (C^{16}), 28.30 (C^{12}), 26.72 (C^7), 18.25 (C^8). ESI-MS: calcd. for $C_{47}H_{74}N_5O_{10}^+$: 868.5430. Found: 868.5428 $[M+H]^+$.

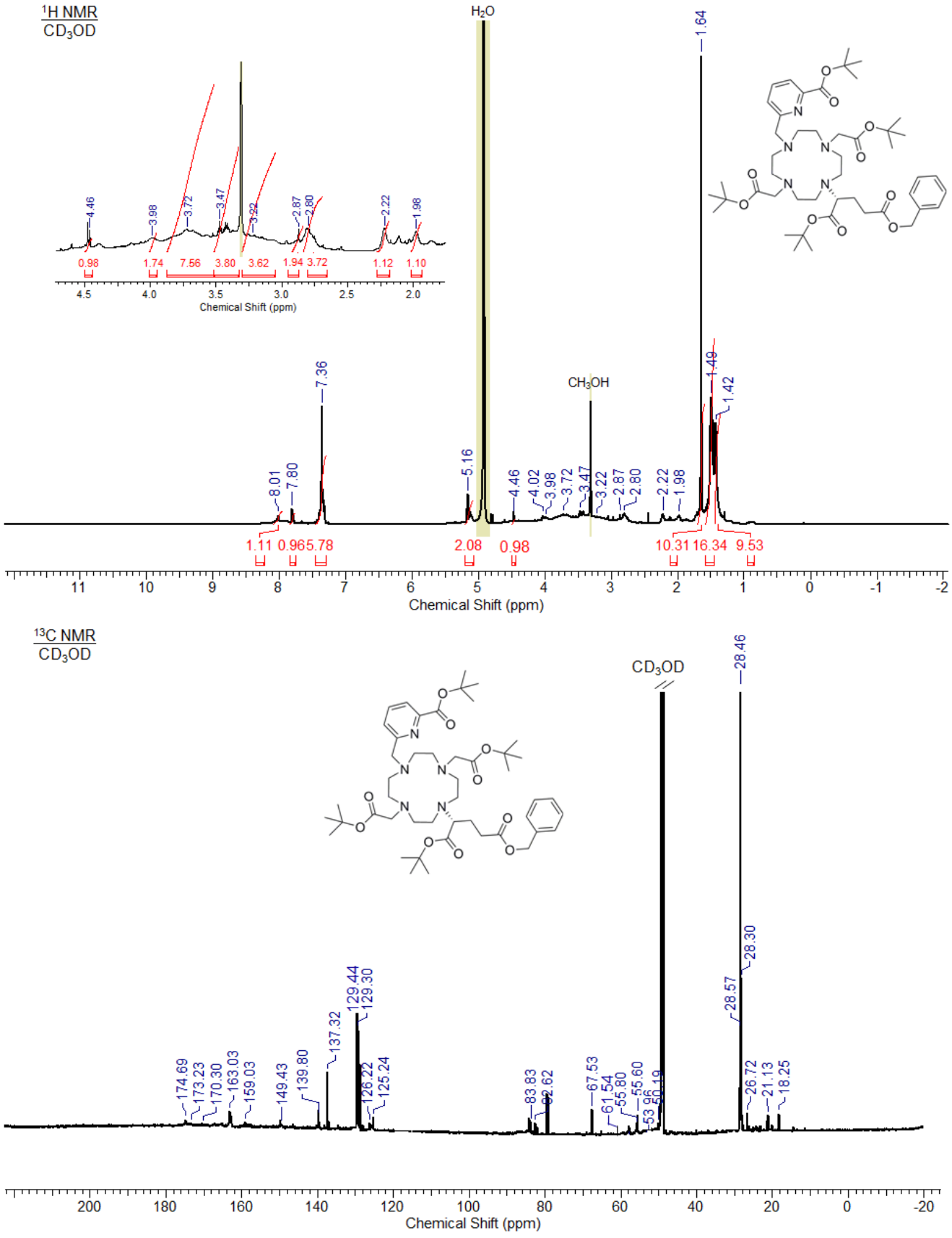

Figure S2. ^{1}H (top) and ^{13}C (bottom) NMR spectra of **4**.

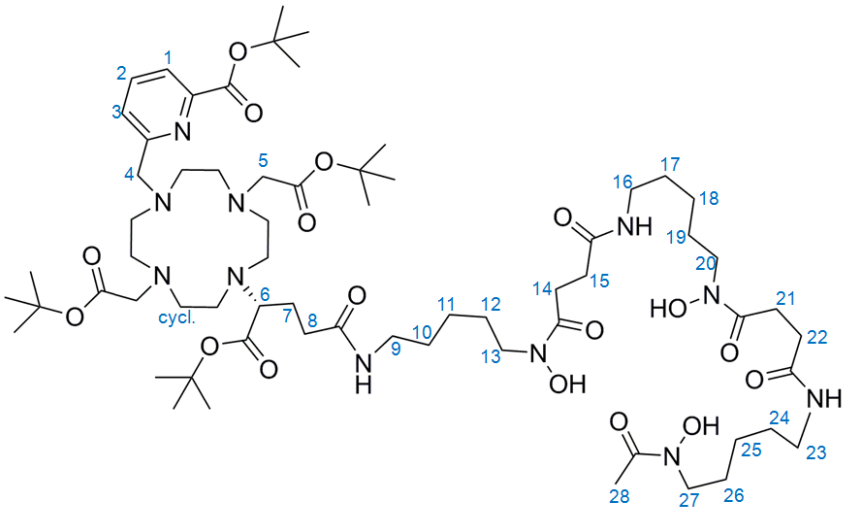

2-(R)-2-(7,10-Bistert-Butyloxycarbonylmethyl-(6-Carboxypyridin-2-yl)tert-butyl)-1,4,7,10-tetraazacyclododec-1-yl)-pentanedioic Acid 1-tert -Butyl Ester,5-(R)-(+)r-desferoxamide, 5. To a solution of **4** (18.2 mg, 0.021 mmol) in MeOH (5 mL), a suspension of Pd/C catalyst (10% w/w, 2.5 mg) in MeOH (5 mL) was added. The flask was evacuated, charged with H_2 (1 atm), and then stirred for 3 h, until no more starting material was detected according to LC-MS. The reaction mixture was filtered, and the volatiles were removed from the filtrate to afford the debenzylated product as white powder (11.7 mg, 0.015 mmol, 72% yield, ESI-MS: calcd. for $C_{40}H_{68}N_5O_{10}^+$: 778.4961. Found: 778.4975 $[M+H]^+$, R_t (method C) =7.55 min). Without further purification, this compound was then dissolved in 1 mL of DMF. DFO-mesylate (16.1 mg, 0.024 mmol), HBTU (9.0 mg, 0.025 mmol) and diisopropylethylamine (3.6 μL) were added to this solution, and the reaction mixture was stirred at 40ºC for 12 hours. The solution was purified using HPLC (method A), with **5** eluting at 17.1 minutes. The fractions containing product were pooled, the solvent was removed in vacuo and **5** was obtained as white solid (7.9 mg, 0.0060 mmol, 40% yield, R_t (method C) =7.82 min). ^{1}H NMR (CD_3OD, 700 MHz): δ 8.02 (m, 1H, H^3), 7.80 (m, 1H, H^2), 7.27 (m, 1H, H^4), 4.38 (m, 1H, H^8), 3.98 (s, 2H, H^5), 3.60 (m,8H, H^{cycl}), 3.55 (m, 6H, $H^{16,cycl}$), 3.50 (m, 4H, $H^{23,30}$), 3.21 (m, 4H, H^{cycl}), 3.16 (m, 6H, $H^{12,19,26}$), 3.07 (m, 2H, H^{11}), 2.76 (m, 4H, $H^{17,24}$), 2.64 (br. s, 4H, H^6), 2.45 (m, 4H, $H^{18,25}$), 2.23 (m, 1H, H^{10}), 2.09 (s, 3H, H^{31}), 1.99 (m, 1H, H^{10}), 1.64 (m, 15H, H^9, $H^{15,22,29}$), 1.56 (m, 21H, H^7, $H^{13,20,27}$), 1.44 (m, 12H, H^1, $H^{13,20,27}$), 1.33 (m, 6H, $H^{14,21,28}$). ESI-MS: calcd. for $C_{65}H_{114}N_{11}O_{17}^+$: 1320.8389. Found: 1320.8400 $[M+H]^+$.

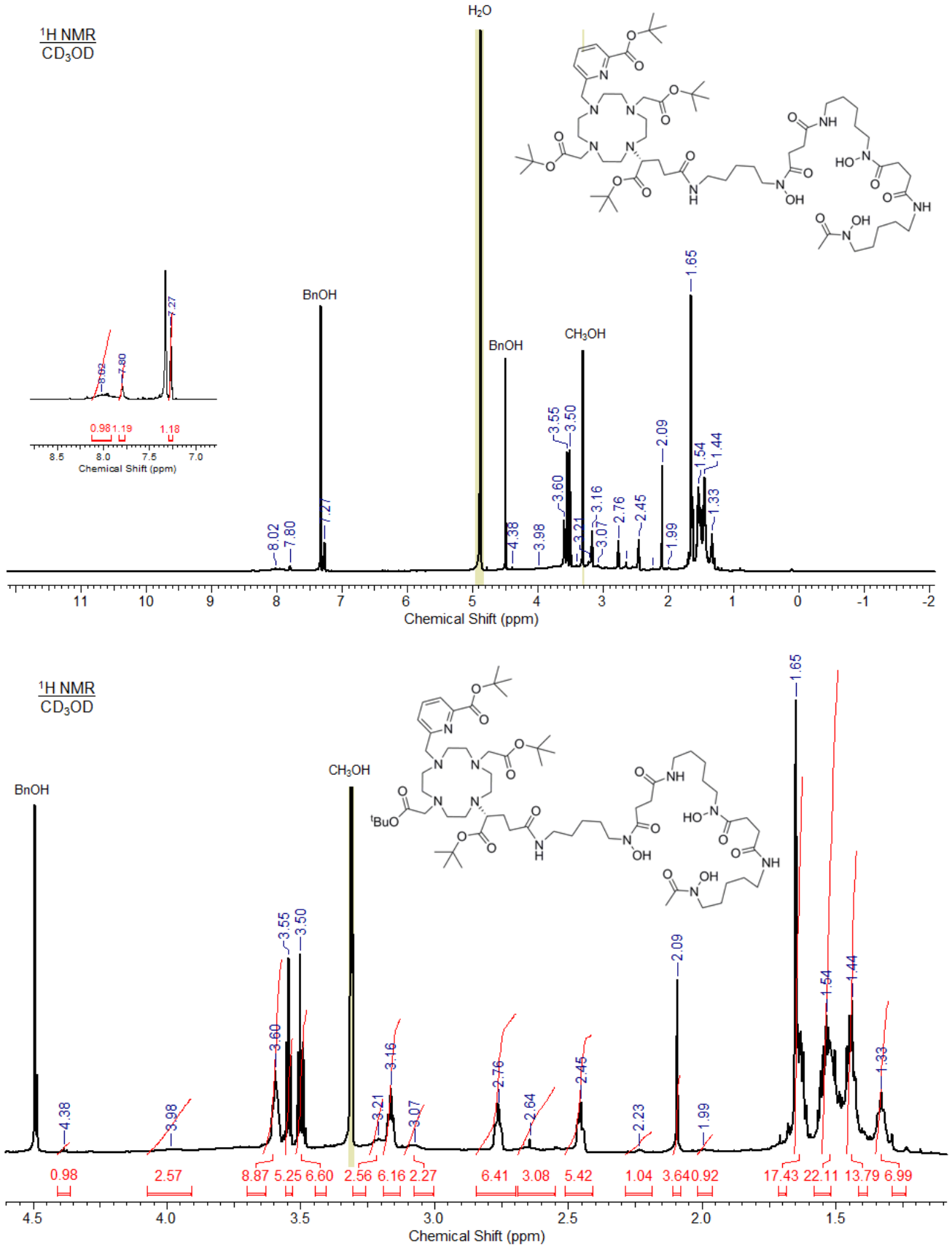

Figure S3. ^{1}H NMR spectrum of **5** (top) with an expansion of the alkyl region (bottom).

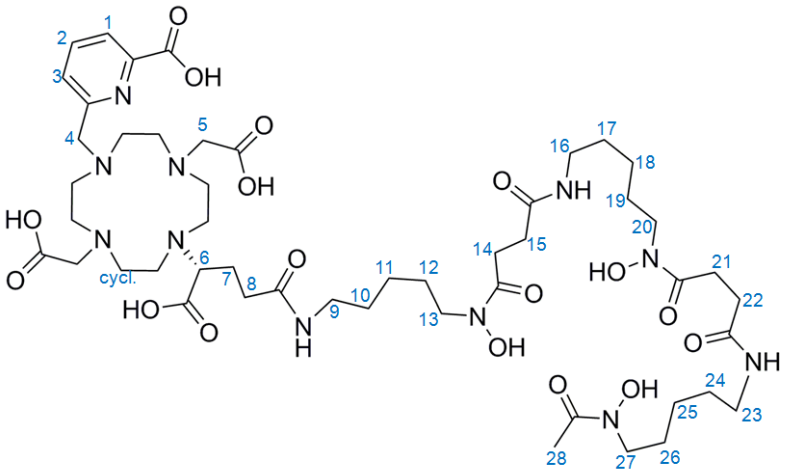

2-(R)-2-(7,10-Bis-carboxycarbonylmethyl-(6-Carboxypyridin-2-yl)-1,4,7,10-tetraazacyclododec-1-yl)-pentanedioic Acid, 5-(R)-(+)r-desferoxamide, L2. 5 (7.9 mg, 0.006 mmol) was dissolved in 1:1 solution of TFA and DCM (1 mL), and stirred for 20 hours. The solvent was removed in vacuo, and the product was redissolved in H_2O. The solution was then lyophilized to yield **L2** as a white powder (5.6 mg, 0.005 mmol, 85% yield, R_t (method C) = 8.95 min). This material was used without further purification for Tb (III) complexation. However, for characterization of the compound, a sample was purified using HPLC (method A), with **L2** eluting at 9.6 minutes. ^{1}H NMR (CD_3OD, 700 MHz): δ 8.01 (m, 1H, H^2), 7.89 (m, 1H, H^1), 7.33 (m, 1H, H^3), 4.38 (t, 1H, H^6), 3.92 (br. s, 2H, H^4), 3.68 (m, 4H, H^{cycl}), 3.60 (m, 8H, H^{cycl}), 3.55 (m, 2H, H^{13}), 3.50 (m, 4H, $H^{20,27}$), 3.41 (m, 2H, H^{cycl}), 3.20 (m, 4H, $H^{8,cycl}$), 3.16 (m, 6H, $H^{9,16,23}$), 2.76 (m, 4H, $H^{14,21}$), 2.70 (s, 4H, H^5), 2.46 (m, 4H, $H^{15,22}$), 2.09 (s, 3H, H^{28}), 1.73 (m, 2H, H^7), 1.63 (m, 6H, $H^{12,19,26}$), 1.53 (m, 6H, $H^{10,17,24}$), 1.33 (m, 6H, $H^{11,18,25}$). ESI-MS: calcd. for $C_{49}H_{82}N_{11}O_{17}^+$: 1096.5890. Found: 1096.5891 $[M+H]^+$.

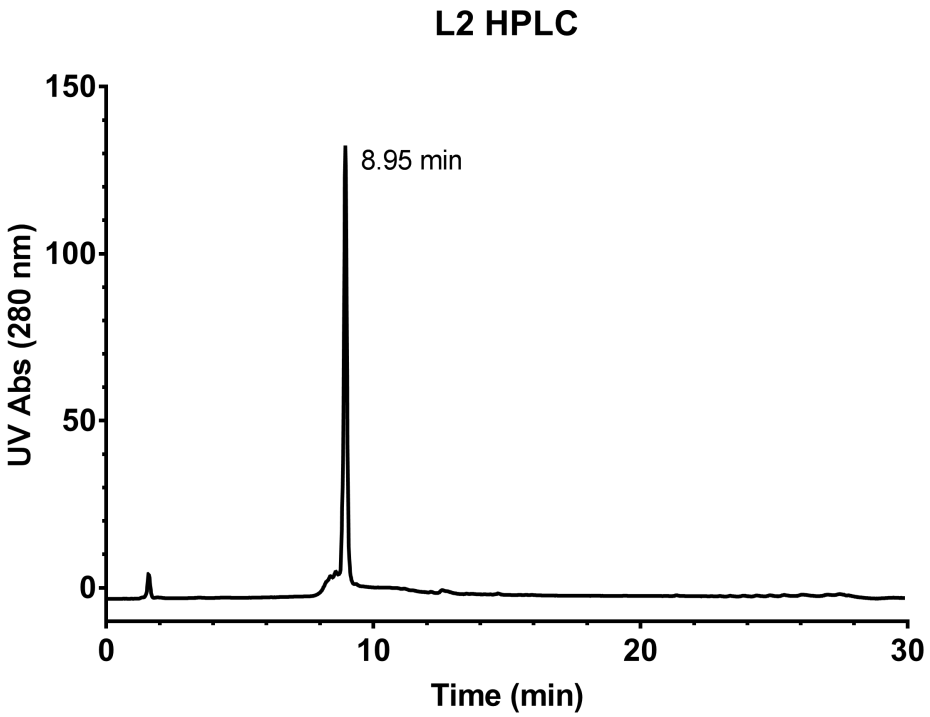

Figure S4. HPLC chromatogram of **L2** (λ=280 nm).

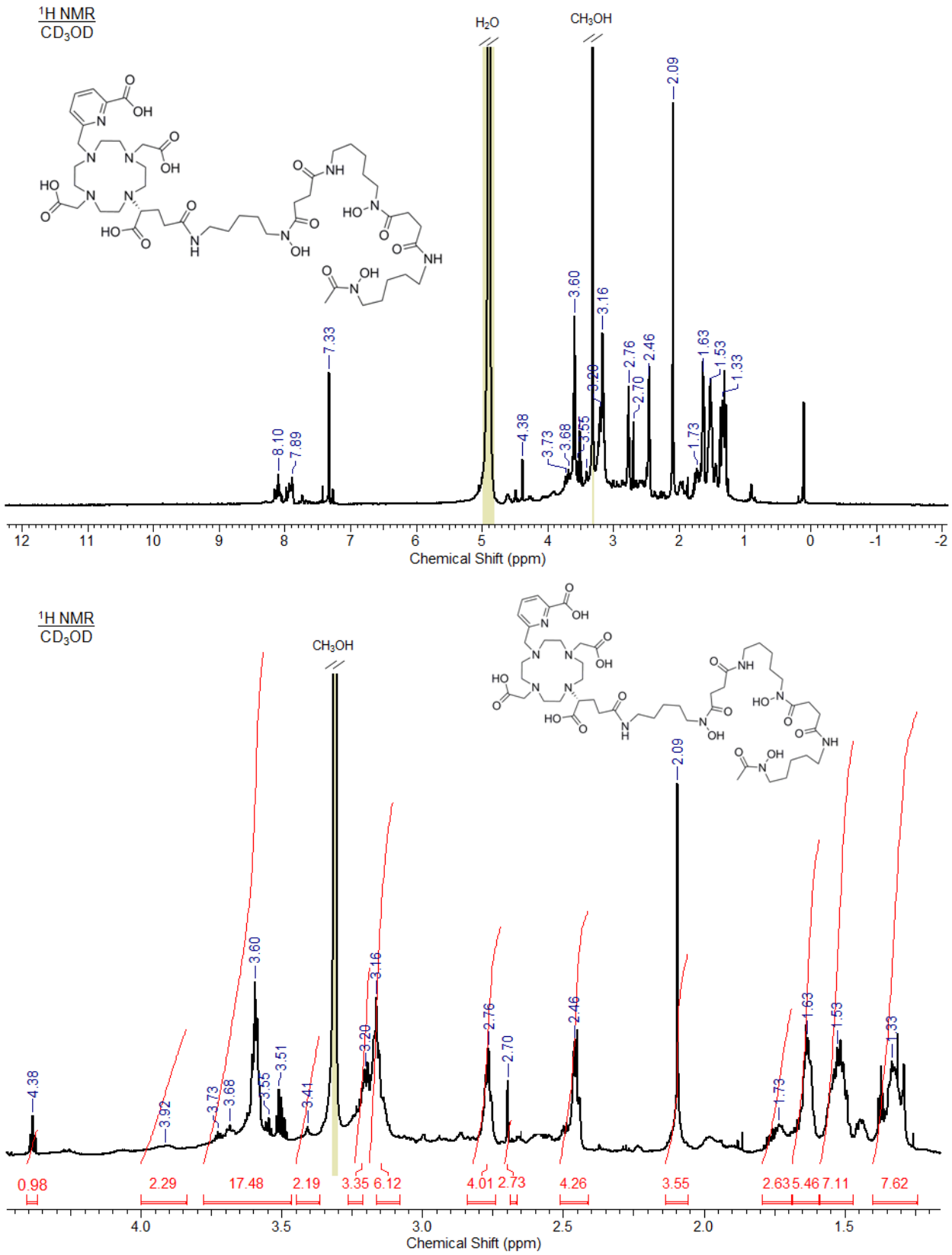

Figure S5. ^{1}H NMR spectrum of **L2** (top) with an expansion of the alkyl region (bottom).

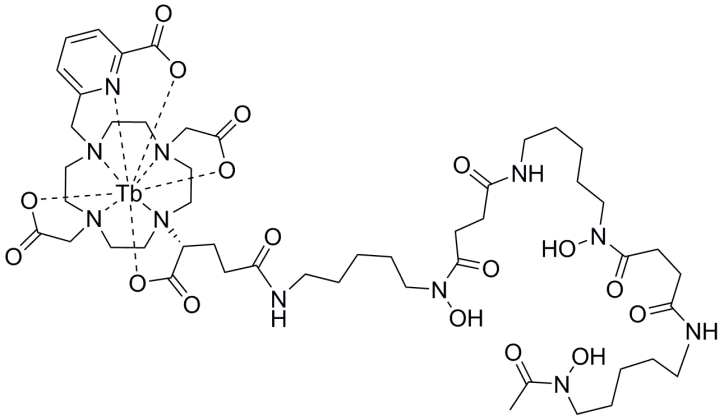

[Tb(**L2**)]$^-$. **L2** (5.6 mg, 0.0051 mmol) was dissolved in 400 μL of H_2O, followed by the addition of 1M NaOH (20 μL). 3 mg of $Tb(OTf)_3$ (0.0051 mmol) dissolved in 500 μL of H_2O was added to this solution. The pH was adjusted to 7 using 1M NaOH. Complexation of Tb (III) was observed by enhanced fluorescence emission under hand-held UV-lamp and confirmation of the desired mass via MS. SepPak purification (Waters Sep-Pak C18 Plus Short Cartridge, 360 mg Sorbent per Cartridge, 55-105 μm Particle Size) was performed to remove Na_3OTf, and the product eluted at 80:20 (H_2O:MeCN) fraction. The fractions containing the product were pooled and lyophilized, and [Tb(**L2**)]$^-$ was obtained as white solid (3.4 mg, 0.0027 mmol, 52% yield). Upon observing the presence of impurities on the HPLC trace, further purification was performed using method B, and the product eluted at 8.65 min. A different sample of [Tb(**L2**)]$^-$ was purified using method C (R_t: 8.90 min, started collection from 8.65 min). ESI-MS: calcd. for $C_{49}H_{77}N_{11}O_{17}Tb^-$: 1250.4758. Found: 1250.4763 [M]$^-$.

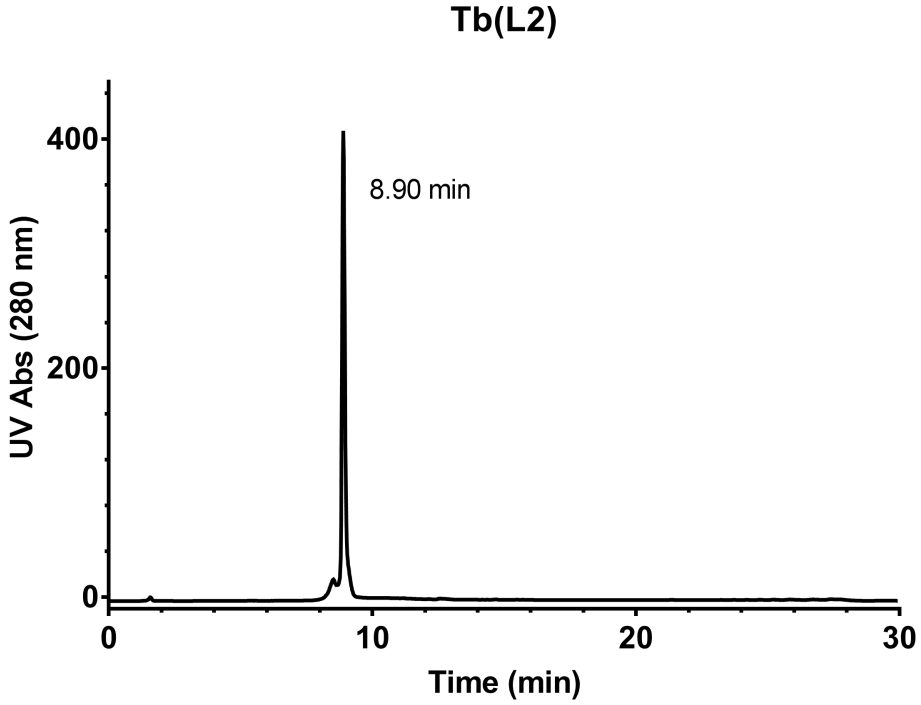

Figure S6. HPLC chromatogram of [Tb(**L2**)]$^-$ (λ=280 nm)

Radiolabeling: Zirconium-89 ($t_{1/2}$ = 78.4 h) was provided by University of Wisconsin-Madison in the form of ^{89}Zr(oxalate)$_4$. The pH of the solution was adjusted to 7-7.5 with sodium carbonate (0.1 M solution). Concentration series of [Ln(DOTA**)]**$^-$, [Ln(**L1**)]$^-$, or [Tb(**L2**)]$^-$ were aliquoted with 10 µCi of pH-adjusted ^{89}Zr. HPLC was used to analyze [Tb(**L2**)]$^-$ for quantitative labeling. Fluorine-18 was in the form of ^{18}F-Kryptofix (Stony Brook Medicine). The ^{18}F ($t_{1/2}$ = 109 min) isotope solution was diluted to an adequate activity per volume with 1X DPBS buffer. Concentration series of [Ln(DOTA**)]**$^-$ or [Ln(**L1**)]$^-$ were doped with 10 µCi of activity. Additional experiments with higher activities (see Figures **S14**, **S15**, **S16**) of either isotope were also doped with ratiometric amounts of activity.

4. Absorption and Emission Spectra

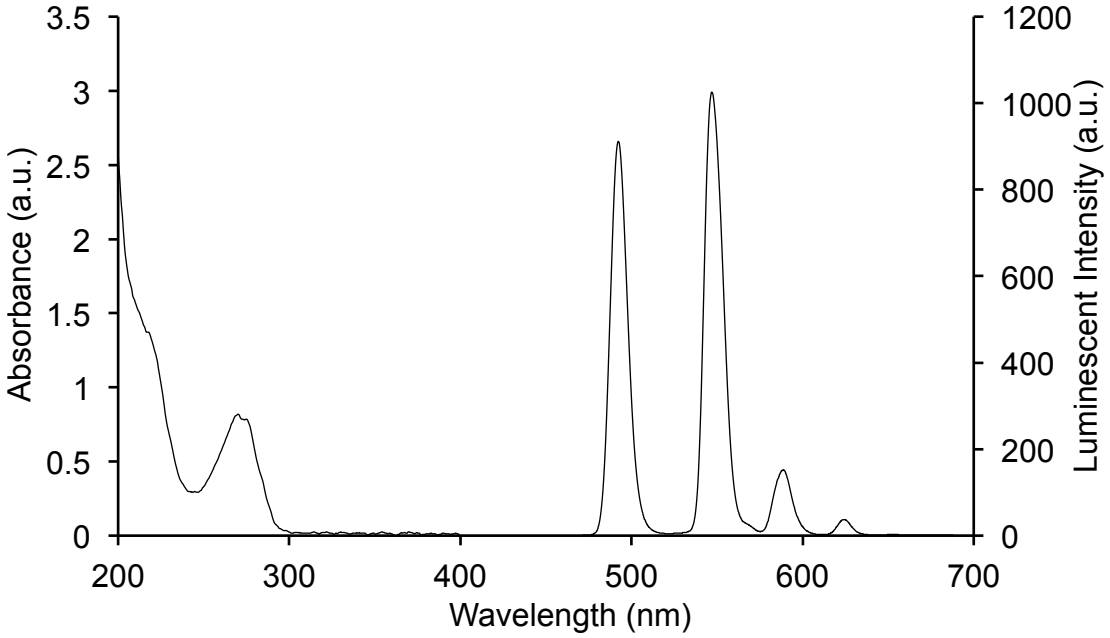

Figure S7. Absorption (UV) and emission (fluorescence) spectra of the [Tb(**L1**)]$^-$ complex in H_2O. Maximum absorbance at 275 nm corresponds to picolinate antenna.

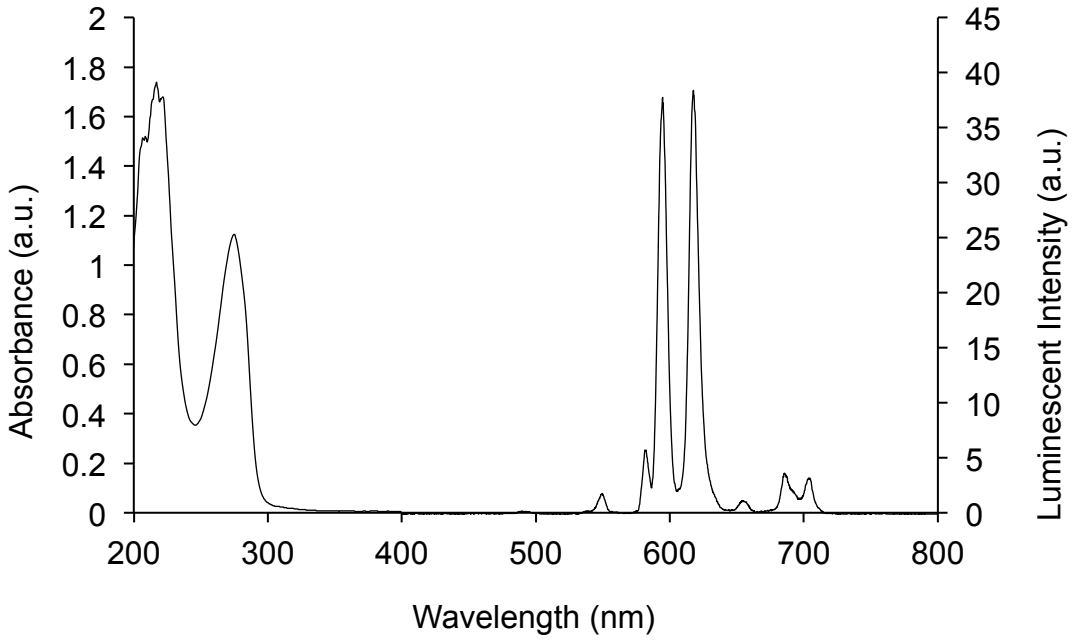

Figure S8. Absorption (UV) and emission (fluorescence) spectra of the [Eu(**L1**)]$^-$complex in H_2O. Maximum absorbance at 275 nm corresponds to picolinate antenna.

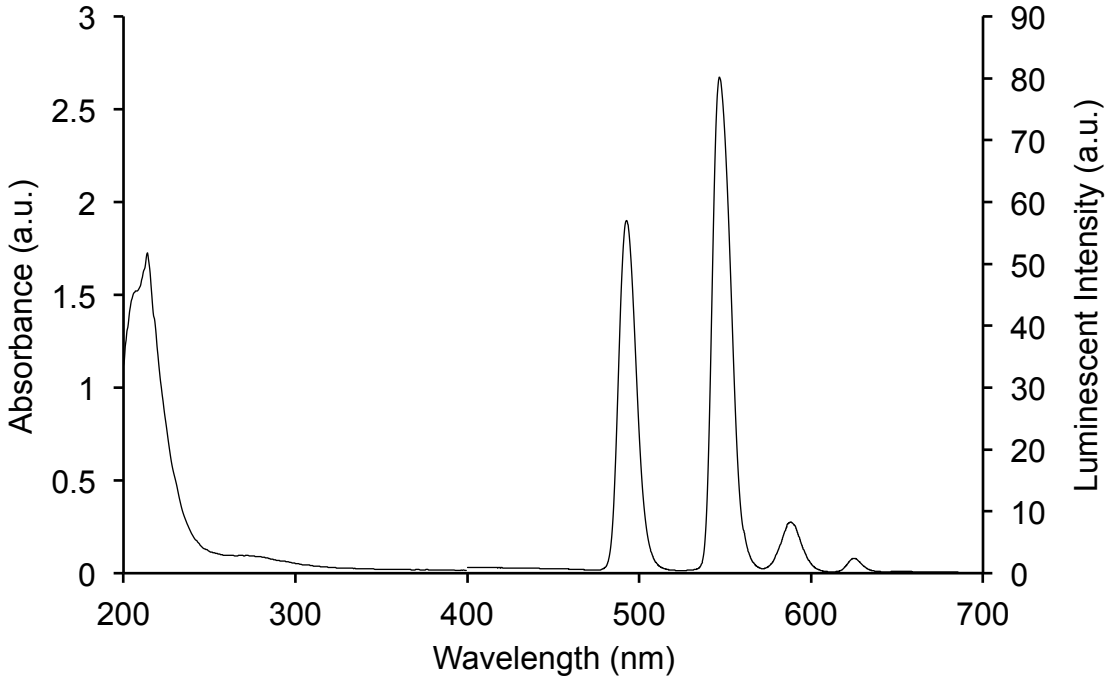

Figure S9. Absorption (UV) and emission (fluorescence) spectra of the $[Tb(DOTA)]^-$ complex in H_2O.

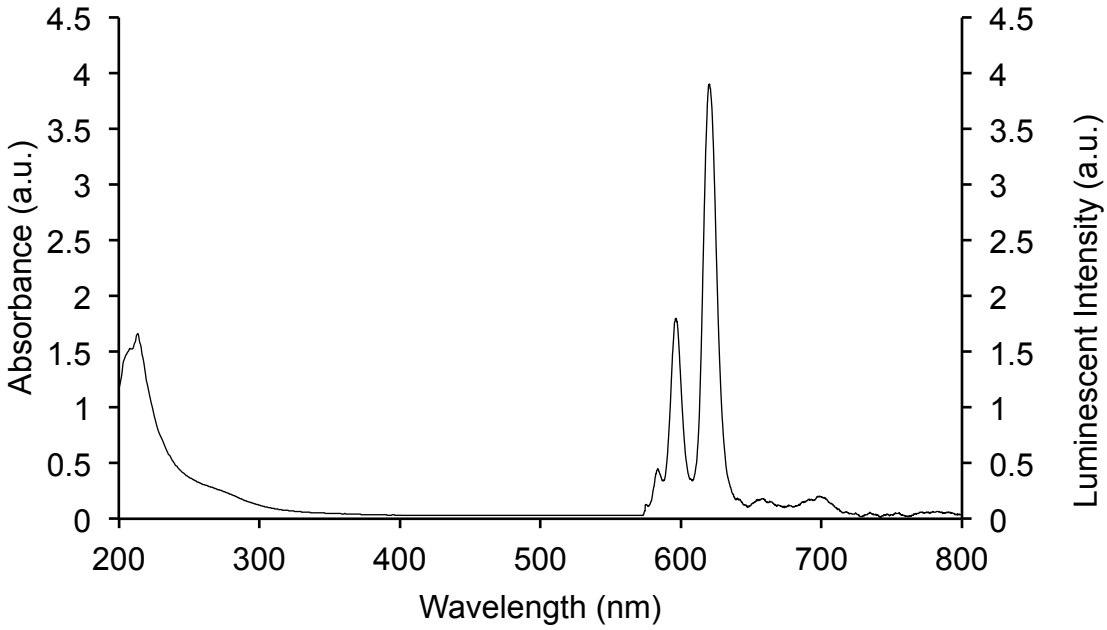

Figure S10. Absorption (UV) and emission (fluorescence) spectra of the $[Eu(DOTA)]^-$) complex in H_2O.

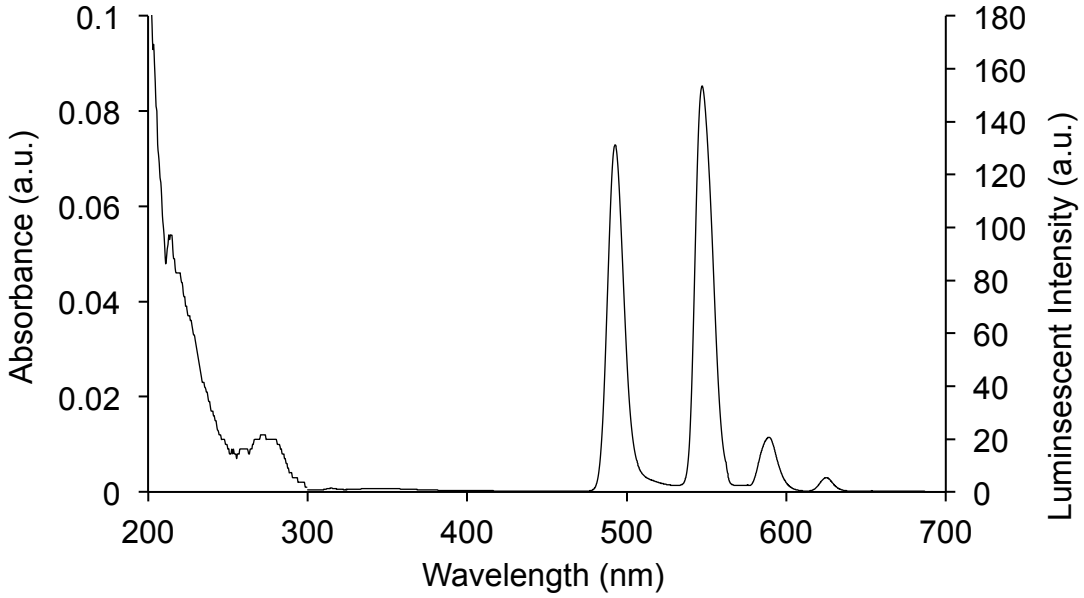

Figure S11. Absorption (UV) and emission (fluorescence) spectra of the [Tb(**L2**)]$^-$ complex in H_2O. Maximum absorbance at 275 nm corresponds to picolinate antenna.

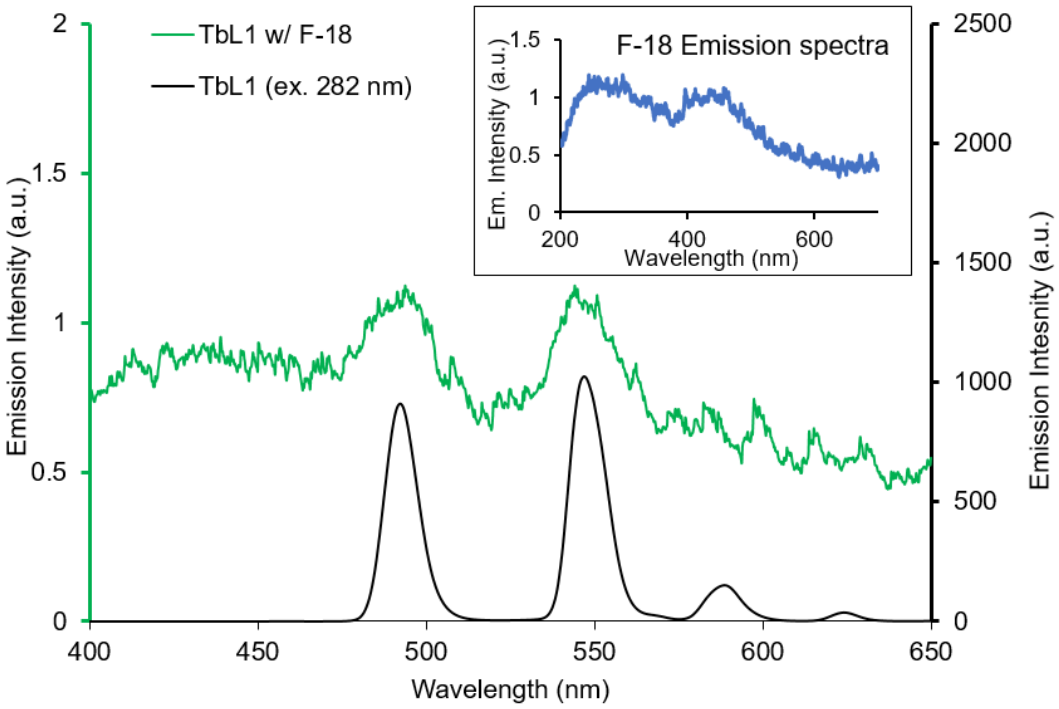

Figure S12. Spectrum collected by standard fluorimeter, with blocked excitation and emission. Blue (inset): Emission continuum of Cerenkov radiation from ^{18}F in DPBS buffer solution (λ_{em} = 200-700 nm). Green (left y-axis): Emission bands of [Tb(**L1**)]$^-$ in presence of 2.2 mCi ^{18}F (λ_{em} = 400-700 nm). Black (right y-axis): [Tb(**L1**)]$^-$ excited by 282 nm wavelength for reference (See Figure S7).

5. Quantum yield and luminescence lifetime measurements

Quantum yield for each complex was determined using the following equation:

$$QY_X = QY_S * \frac{Gradient_X}{Gradient_S} \qquad \text{eq. 1}$$

where "S" refers to the inorganic fluorophore $Ru(bipy)_3$ standard (Φ = 0.042) and "X" is the unknown. The gradient is the slope of the graph of integrated emission intensity versus the peak absorption value for a range of concentrations. Lifetime values were extracted by fitting the luminescent decay curves with the equation:

$$I_t = I_0 * \exp\left(-\frac{x}{\tau}\right) \qquad \text{eq. 2}$$

where I_t is the initial luminescent emission intensity, I_0 is the intensity at time x = 0, and τ is the luminescence lifetime. Data was fit using Igor. Q was calculated using Horrocks' method, eq. 3.

$$q = A\left(\frac{1}{\tau(H_2O)} - \frac{1}{\tau(D_2O)}\right) \qquad \text{eq. 3}$$

where A = 5.0 and 1.2 ms^{-1} for Tb^{3+} and Eu^{3+} respectively.[3]

Table S1. Lifetime values (**τ**, ms) for complexes evaluated.

	[Tb(**L1**)]$^-$	[Eu(**L1**)]$^-$	[Tb(DOTA)]$^-$	[Eu(DOTA)]$^-$	[Tb(**L2**)]$^-$
H_2O	**2.83**	**2.21**	**1.73**	**1.59**[†]	**1.73**
D_2O	**2.75**	**2.30**	**2.55**	**2.08**[†]	**1.77**

[†] Literature value. See Ref 3.

6. IVIS phantom images and ROI radiance quantification

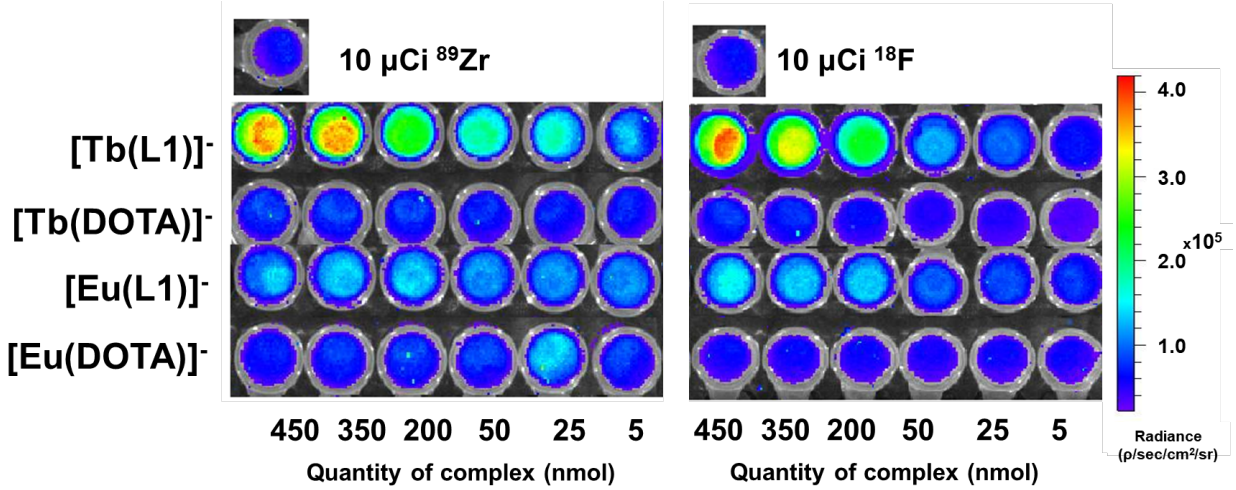

Figure S13. IVIS open emission images of complexes (5-450 nmol) doped with 10 µCi of ^{89}Zr (left) or ^{18}F (right).

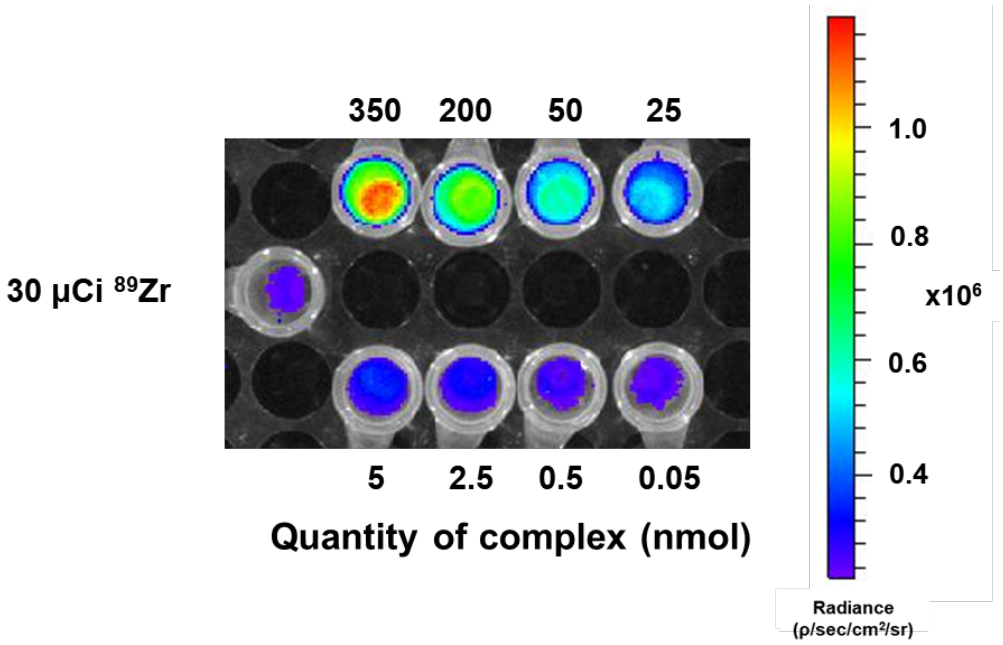

Figure S14. IVIS open emission images of [Tb(**L1**)]$^-$ at 0.05-350 nmol with 30 µCi of ^{89}Zr. Note larger radiance scale.

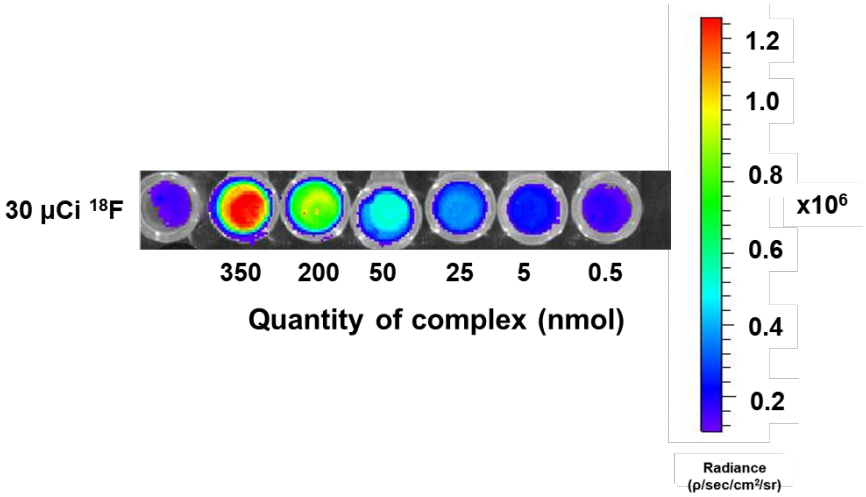

Figure S15. IVIS open emission images of [Tb(**L1**)]$^{-}$ at 0.5-350 nmol with 30 µCi of ^{18}F. Note larger radiance scale.

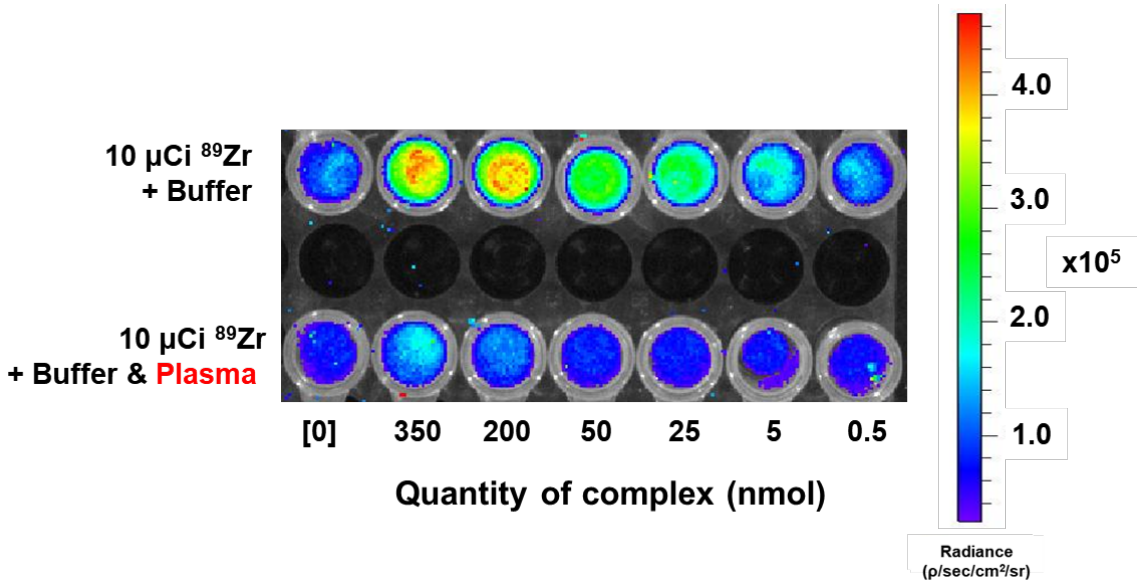

Figure S16. IVIS open emission images of [Tb(**L1**)]$^{-}$ with and without added plasma at 0.5-350 nmol with 10 µCi of ^{89}Zr.

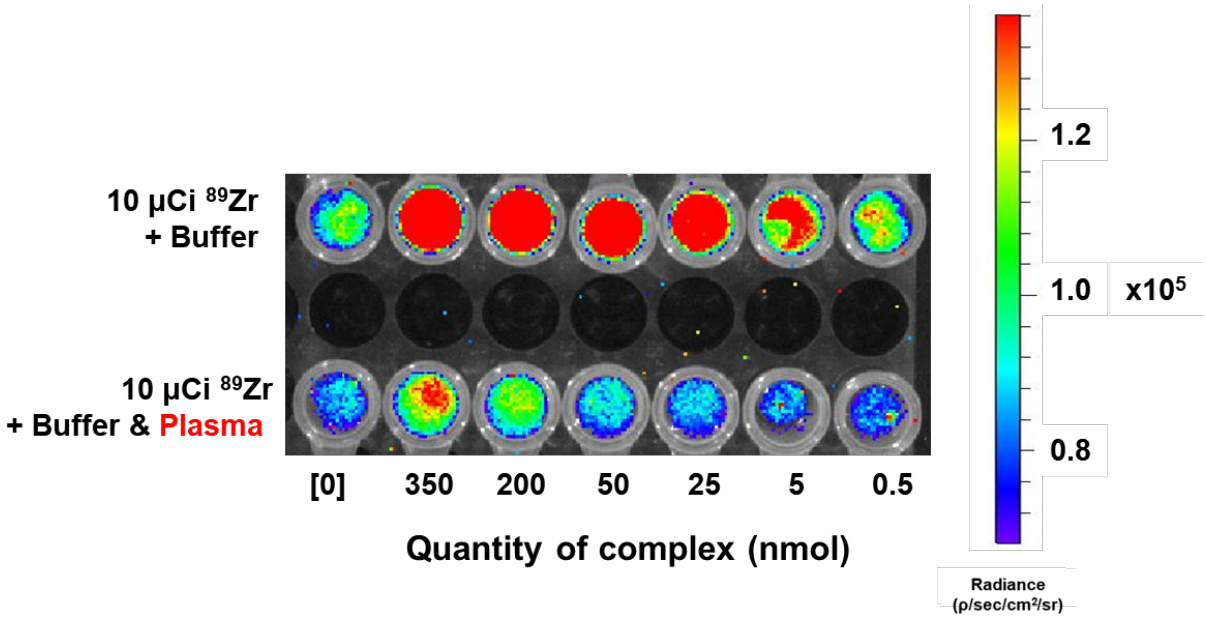

Figure S17. IVIS open emission images of [Tb(**L1**)]$^-$ with and without added plasma at 0.5-350 nmol with 10 µCi of ^{89}Zr. Note shifted windowing, which allows for visualization of concentration gradient containing plasma.

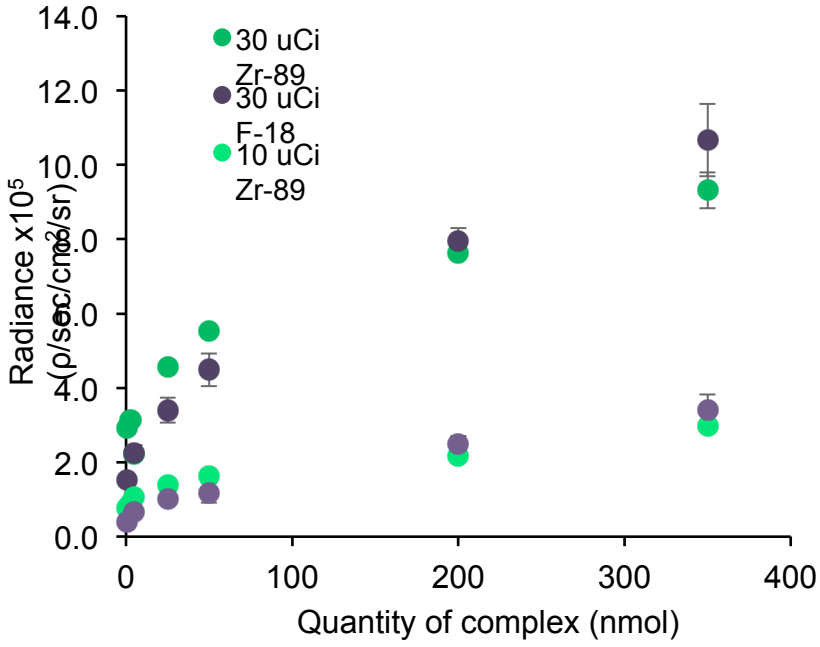

Figure S18. ROI quantification of radiance from IVIS open emission images (Figures **S13, S14, S15**). Shown as a function of quantity of complex of [Tb(**L1**)]$^-$ with 10 and 30 µCi of either ^{18}F or ^{89}Zr. n=5.

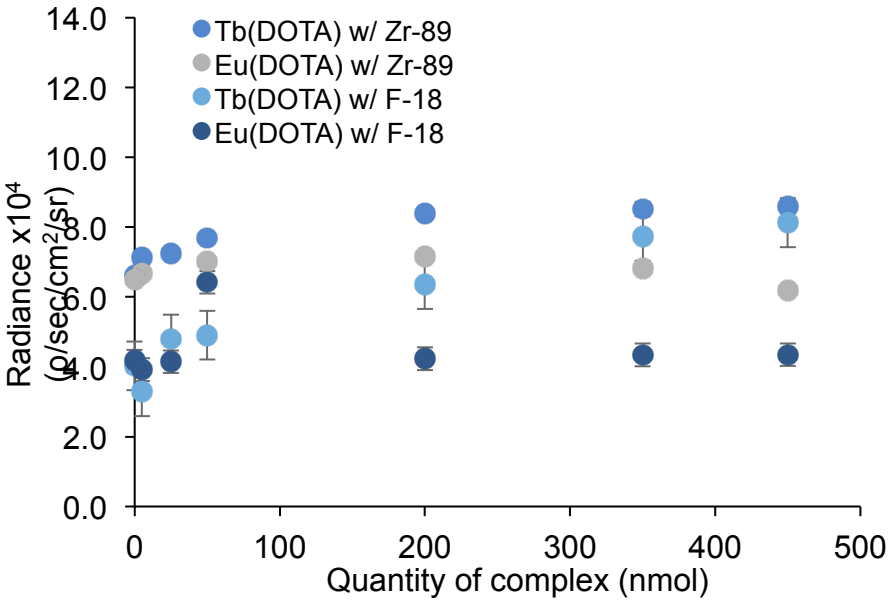

Figure S19. ROI quantification of radiance from IVIS open emission images (Figure **S13**). Shown as a function of quantity of complex of $[Tb(DOTA)]^-$ and $[Eu(DOTA)]^-$ with 10 µCi of either ^{18}F or ^{89}Zr. n=5.

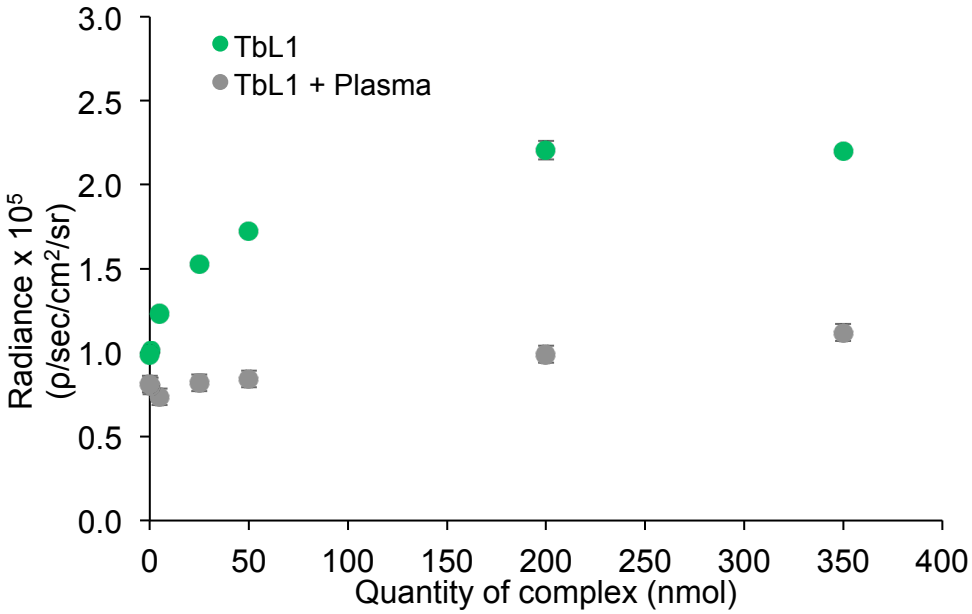

Figure S20. ROI quantification of radiance from IVIS open emission images (Figure **S16/S17**). Shown as a function of quantity of complex of $[Tb(\mathbf{L1})]^-$ with added rat plasma with 10 µCi of ^{89}Zr. n=5.

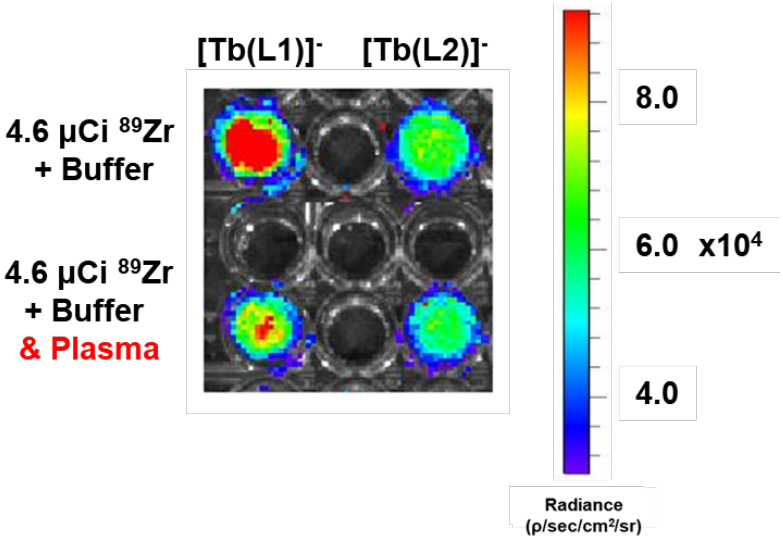

Figure S21. IVIS open emission images of [Tb(**L1**)]$^-$ and [Tb(**L2**)]$^-$ with and without added plasma at 100 nmol with 4.6 µCi of ^{89}Zr.

[La(L1)]- 10 µCi ^{89}Zr

Quantity (nmol)	Average Radiance	Stdev
600	70441	4153
450	72301	2029
350	63826	1422
200	72509	2281
50	82657	3396
25	83001	2489
5	72235	2654
0	69838	2708

[Tb(**L2**)]$^-$ 10 µCi ^{89}Zr

Quantity (nmol)	Average Radiance	Stdev
10	110966	1875
2.5	107333	1500
1	99901	1299
0.5	91549	998
0.1	89673	2906
0	86721	1863

[Tb(**L1**)]$^-$ 30 µCi ^{18}F

Quantity (nmol)	Average Radiance	Stdev
450	1123122	97015
350	1065722	34237
200	795462	44199
50	449002	33409
25	340102	19358
5	226602	12063
0.5	153562	11297
0	129262	10537

[Tb(**L1**)]$^-$ 10 µCi ^{18}F

Quantity (nmol)	Average Radiance	Stdev
450	376336	52138
350	340761	40974
200	250687	19423
50	117784	26835
25	102399	4977
5	66225	3465
0.5	40182	2363
0	33918	1685

[Tb(**L1**)]$^-$ 10 µCi ^{89}Zr

Quantity (nmol)	Average Radiance	Stdev
450	83879	961
350	85603	2309
200	78389	1309
50	81373	3043
25	84409	779
5.0	77771	2402
0.00	71418	1958

[Tb(**L1**)]$^-$ 10 µCi ^{89}Zr

Quantity (nmol)	Average Radiance	Stdev
10	121199	10263
2.5	105299	2986
1	95791	2732
0.5	87431	1981
0.1	83303	2355
0	86721	1863

[Tb(**L1**)]$^-$ 30 µCi ^{89}Zr

Quantity (nmol)	Average Radiance	Stdev
350	930963	48669
200	763313	10910
50	552763	10890
25	456413	10378
5	221788	3478
2.5	314163	2903
0.5	290513	3930
0.05	246763	3645
0	238113	1810

*Radiance measured in ρ/cm^2/sec/sr.

[Tb(**L1**)]$^-$ 10 µCi ^{89}Zr (Figure S20)			[Tb(**L1**)]$^-$ 10 µCi ^{89}Zr + plasma		
Quantity (nmol)	Average Radiance	Stdev	Quantity (nmol)	Average Radiance	Stdev
350	219796	2498	350	111921	2476
200	220521	5608	200	98971	1030
50	172371	1326	50	84359	739
25	152696	2455	25	82051	617
5	123121	952	5	73769	1189
0.5	101071	792	0.5	80199	932
0	98921	874	0	81334	705

Table S2. *Radiance measured in ρ/cm^2/sec/sr.

Table S3. Quantity = 100 nmol, with 4.6 µCi of ^{89}Zr

	Complex without plasma		Complex with plasma		
	Radiance	Stdev	Radiance	Stdev	% Change of radiance upon addition of plasma
[Tb(**L1**)]$^-$	76341	936	47831	2411	-37%
[Tb(**L2**)]$^-$	48481	1395	44584	303	-8%

*Radiance measured in ρ/cm^2/sec/sr.

7. References

[1] Regueiro-Figueroa, M. et al. *Inorg. Chem*. 2011, 50 (9), 4125-4141.

[2] Umegawa, Y. et al. *Magn. Reson. Chem*. 2016, 54 (3), 227-233.

[3] Levy, S. et al. *Org. Process Res. Dev.* 13 (3), 535-542

[4] Beeby, A. et al. *J. Chem. Soc., Perkin Trans*. 2, 1999, 493-503.